

## Application of Satellite Thermal Infrared Imagery to Geothermal Exploration in East Central California

Mariana Eneva<sup>1</sup>, Mark Coolbaugh<sup>2</sup>, and Jim Combs<sup>3</sup>

<sup>1</sup>Imageair, Inc., San Diego, CA • [meneva@imageair-inc.com](mailto:meneva@imageair-inc.com))

<sup>2</sup>Great Basin Center for Geothermal Energy, University of Nevada, Reno, NV [mfc@unr.nevada.edu](mailto:mfc@unr.nevada.edu))

<sup>3</sup>Geo Hills Associates, Reno, NV • [geohills@mac.com](mailto:geohills@mac.com))

### Keywords

*Geothermal, remote sensing, thermal infrared, TIR, satellite, Coso*

### ABSTRACT

The main incentives for use of remote sensing in geothermal exploration are cost-effectiveness and large-area coverage. We analyzed spaceborne thermal infrared (TIR) imagery from the spaceborne ASTER instrument in search for thermal anomalies associated with geothermal resources in the central part of eastern California. We present results from the known geothermal area of the Coso Geothermal Power Project, with emphasis on correction of thermal effects caused by topography and albedo. Taking these effects into account reduces noise and reveals thermal anomalies which are weak or not distinguishable in the uncorrected imagery. In future work, we will look for similar anomalies in unexplored areas and will seek to validate the remote sensing observations with field measurements.

### Background

Remote sensing data can be used as a cost-effective tool to explore large areas for geothermal potential and pinpoint smaller target areas for further exploration using more expensive airborne or ground-based surveys. Recent advances in thermal infrared (TIR) remote sensing open new opportunities for geothermal exploration. We process and analyze images collected by the Advanced Spaceborne Thermal Emission and Reflection Radiometer (ASTER), focusing on the region between the Coso Geothermal Power Project (Monastero, 2002) and the Mammoth Geothermal Power Project located in the central part of eastern California (Figure 1). This region of east central California is suspected to have significant geothermal resources; however, due to the lack of access infrastructure, there has been little geothermal exploration conducted in the region. The purpose of our study has been to identify the thermal signatures

of known geothermal sites and subsequently search for similar features in basically unexplored areas. This is important in view of the increasing interest in electricity generation from renewable resources and, in particular, tapping into the potential 4,000 megawatts of additional power from geothermal energy in California (Sass and Priest, 2002).

### Geothermal Potential in the Western U.S.

Based on current projections, the U.S. will need to increase its current electrical power generating capacity by 40% (~300,000 MWe) over the next 15 years (Williams, 2002). The

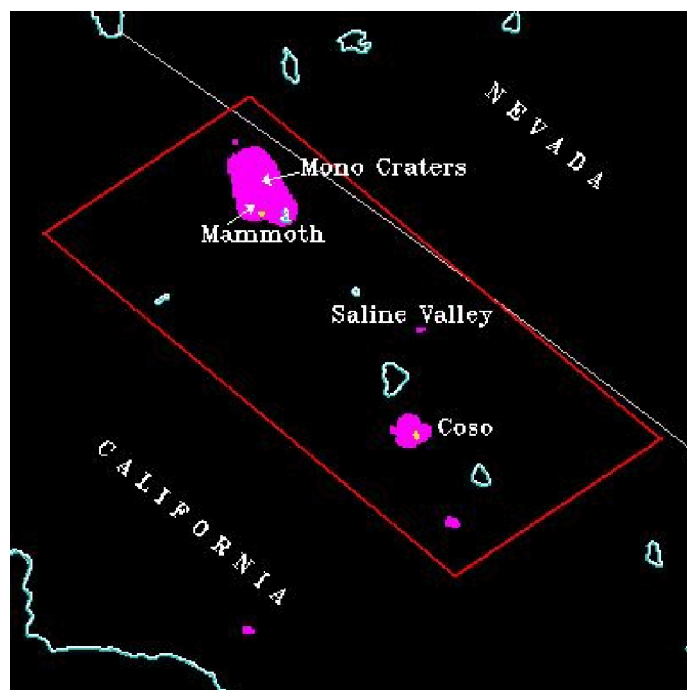


**Figure 1.** Map of geothermal resources in eastern California. Known geothermal resources areas (KGRAs) are shown in pink. Two production areas (in Coso and Mammoth) are shown in yellow in the midst of the KGRAs. Polygon outlined in red is study region.

U.S. Geological Survey has estimated that there is a potential for about 22,000 MWe of electrical power generation in the western U.S. from identified high-temperature (>150°C) geothermal systems at depths less than 3 km. Estimates of potential geothermal power production from undiscovered resources range between 72,000 and 127,000 MWe. Spaceborne remote sensing is particularly cost-effective in the search for new geothermal resources, as long as attributes associated with geothermal fields can be identified.

## Remote Sensing Studies in Geothermal Fields

Attributes to search for with TIR remote sensing are related to high heat flow anomalies, excess vertical temperature gradients, and surface thermal manifestations. Some surface features above geothermal reservoirs are obviously hot, such as geysers, hot springs, fumaroles, and mud pools. Less obvious surface attributes of geothermal fields amenable to TIR remote sensing include locally elevated temperatures, geobotanical characteristics (e.g., thermally stressed vegetation), bare altered ground, host rock permeability and topographic relief, and the presence of certain rock types and minerals.

Previous applications of optical and infrared remote sensing to geothermal fields, both airborne and spaceborne, have sought to characterize the associated fracture systems and to capture specific surface expressions of the underlying geothermal reservoirs. Multispectral and hyperspectral *airborne* remote sensing has been long used over geothermal areas, including TIR scanning (e.g., Pickles et al., 2001; Allis et al., 1999; Coolbaugh et al., 2000; Martini et al., 2000). Earlier examples of *spaceborne* remote sensing include applications of data from Landsat TM, SPOT XS, and SPOT PAN imagery, at 30-m, 20-m, and 10-m spatial resolution (e.g., Cochrane et al., 1994). Calvin et al. (2002) used day/night ASTER scenes over the Brady Hot Springs geothermal area (Nevada), where they identified a thermal anomaly associated with a nearby fault. Corrections for topographic slope orientation, albedo, and thermal inertia (Coolbaugh et al., 2000; Coolbaugh, 2003) have been shown to increase the number of remotely sensed thermal anomalies by an order of magnitude compared with remote sensing without such corrections.

## ASTER Data

Compared with previous TIR remote sensing, ASTER (<http://asterweb.jpl.nasa.gov/>) provides significantly more possibilities. It is a unique Japanese instrument mounted on the U.S. Terra satellite launched in December 1999. The minimum revisit time interval over any given site is 16 days. ASTER acquires data over a 60-km wide swath and provides multispectral images of the Earth's surface in 14 different bands: (1) three visible and near-infrared (VNIR) channels, with wavelengths between 0.5 and 0.9  $\mu\text{m}$ , at 15-m resolution; (2) six short-wave infrared (SWIR) channels, 1.6 to 2.43  $\mu\text{m}$ , at 30-m resolution; and (3) five thermal infrared (TIR) channels, 8 to 12  $\mu\text{m}$ , at 90-m resolution. The most used ASTER data product is Level 1B (radiance at sensor). Higher-level data products are produced on demand and include surface radiance corrected

for atmospheric effects – AST\_09, reflectance – AST\_07, emissivity – AST\_05, and surface kinetic temperature – AST\_08. Subsequent figures (Figures 2 – 5) show results from Level 1B and AST\_08 data that were ordered from the EOS Data Gateway (<http://edcimswww.cr.usgs.gov>) of the Land Processes Distributed Active Archive Center (LPDAAC).

## Relevance of TIR Remote Sensing to Ground-Based Measurements

When working with satellite TIR data, it is necessary to verify that they correspond to ground-based measurements, and thus meaningfully reflect surface and subsurface processes. Allis et al. (1999) compared shallow soil temperature measurements (at <1-m depth) in the Dixie Valley Geothermal Power Project (Nevada) with airborne TIR imagery, both taken prior to dawn in order to minimize solar heating effects from the previous day. Although the airborne TIR temperatures were on average cooler than the soil measurements, good correlation was observed between the two types of temperatures, indicating that anomalies in soil temperature would likely correspond to distinct anomalies of similar magnitude in the TIR measurements. It remains to be seen if such correspondence will hold for spaceborne data. In the summer of 2006, we will collect ground-based measurements at the Coso Geothermal Power Project, concurrently with the collection of ASTER TIR images.

## Effects of Albedo, Topography, and Thermal Inertia

Albedo and topography are treated together in terms of their influence on the overall amount of energy available for heating. High albedo is related to higher reflectance and less energy remaining for heating. Topographic slope orientation is also very important in that southern slopes receive more of the flux of solar irradiance than the northern slopes. For this reason, we calculated so-called shaded relief from a digital elevation model (DEM); it is a number between 0 and 1, with 1 indicating maximum possible heat flux. Thermal inertia indicates how fast a material gets heated and cools off and is significantly affected by porosity. Low values mean cooling off quickly at night, so thermal inertia can be approximately estimated from day/night pairs of thermal satellite images.

## Heat Energy Model

A simplified heat energy model based on net surface radiation flux  $Q$  was used to correct for albedo and topographic slope, following the methodology described by Coolbaugh (2003):

$$Q \sim (1-A)*M(Z)*\cos Z', \quad (1)$$

where  $Q$  is the net radiation flux at the surface,  $A$  is the ground albedo,  $\cos Z'$  is the cosine of the angle between the surface normal and the sun's rays (calculated as shaded relief),  $Z$  is the zenith angle, and  $M(Z)$  is the atmospheric transmission depending on  $Z$ . The shaded relief can be calculated from the sun's elevation and declination for any given date and time of

a satellite passage. The albedo  $A$  can be obtained from:

$$R = K \cdot A \cdot \cos Z' + b, \quad (2)$$

where  $R$  is taken from the AST\_07 product (surface reflectance) and  $\cos Z'$  is the shaded relief calculated for the moment of satellite passage. The constants  $K$  and  $b$  can be estimated from field measurements, which are absent at the moment, so their values were taken to be 1 and 0, respectively (as would be the case if the AST\_07 imagery were perfectly corrected for atmospheric absorption and scattering effects).

The heat flux equation (1) was integrated over time to model changes in the intensity of light and the position of the sun relative to the topographic slopes over the course of a day:

$$E \sim (1-A) \cdot \sum_i [M(Z)_i \cdot \cos Z'_i \cdot D_i] \cdot \Delta t_i, \quad (3)$$

where  $E$  is the solar energy absorbed per unit area over the course of a day;  $\Delta t_i$  is the time interval for each component of the sum;  $D_i$  is a time decay factor ranging from 0 to 1, which is inversely proportional to the time gap between a given position of the sun and the time the imagery was acquired.

This simplified model accounts approximately for heat dissipation and can be used to calculate pseudo-temperature images to be subtracted from the AST\_08 (surface temperature) daytime and nighttime images. Note that despite cooling off after sunset, the nighttime scenes would be still affected by differential heating during the day. This is especially true because the Terra satellite passes only several hours after sunset in California, and not in the pre-dawn hours.

The effect of thermal inertia can be accounted for by summing the corrected day and night AST\_08 images, using weighing coefficients of 0.25 for the daytime image and 0.75 for the nighttime image (Coolbaugh, 2003), which turns out to be a good approximation of the average over the diurnal cycle.

All images have been orthorectified, using a digital elevation model (DEM) from <http://seamless.usgs.gov>. Orthorectification is important in this case because the surface elevations in the Coso area vary rather significantly, from 720 m to 1550 m.

To evaluate the effect of thermal inertia, it is necessary to use a combination of day- and nighttime scenes that span as short time as possible. In California, the Terra satellite passes around 11 p.m. and 10 a.m. standard Pacific time. The best

possible night/day pair data are separated by about 36 hours. Such pairs are very rare in the existing collection of ASTER data, unless planned in advance, but a suitable day/night pair happened to exist over the Coso Geothermal Power Project. More of these pairs will be collected in the summer of 2006 over the whole region of interest.

### Correction of Surface Temperature (AST\_08) Data

In Figure 2, TIR scenes of size ~60 km x 60 km are shown for the day/night pair, partially covering the Coso Geothermal Power Project. The daytime scene was taken on 08/24/2001,

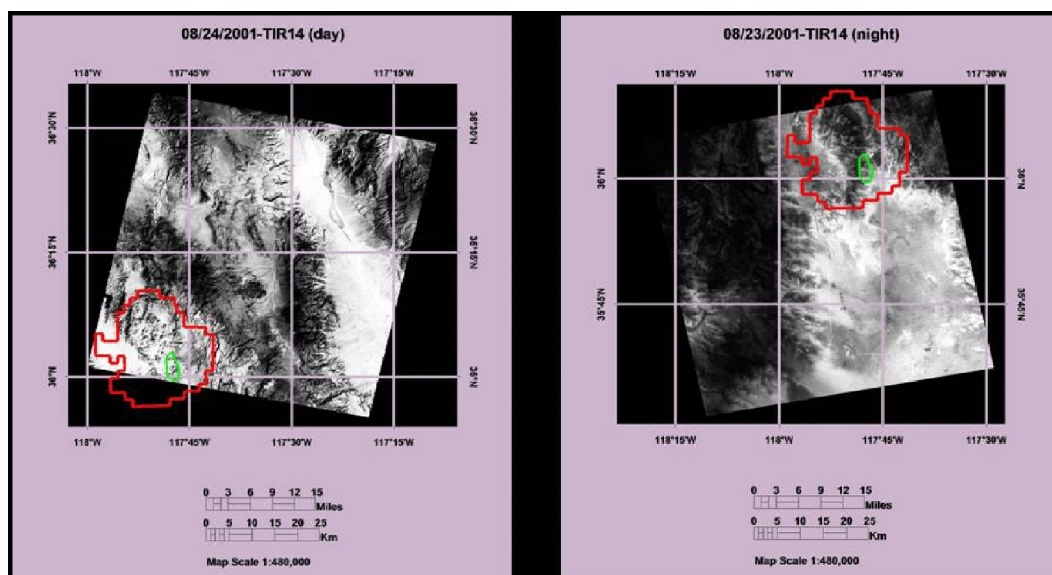


Figure 2. Level 1B TIR band 14, daytime (08/24/2001) and nighttime (08/22/2001) – see text. Coso KGRA and production area are outlined in red and green, respectively.

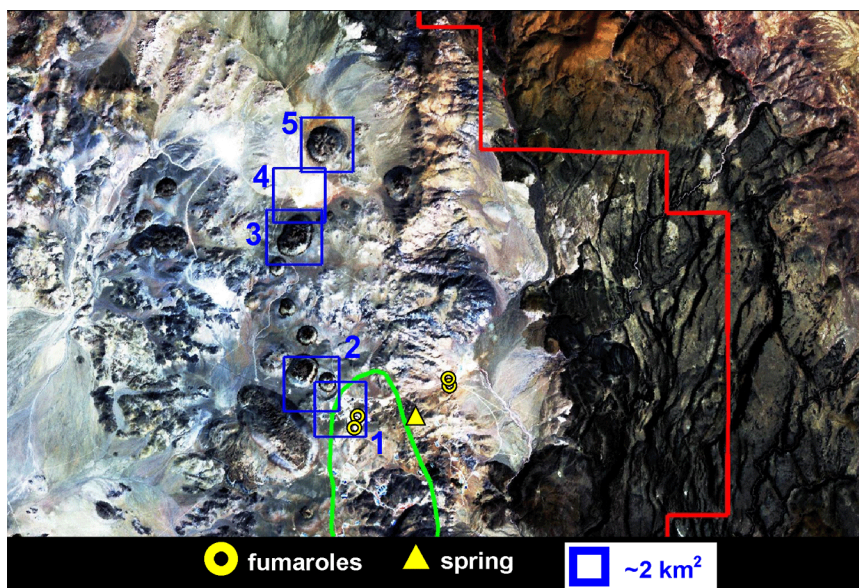
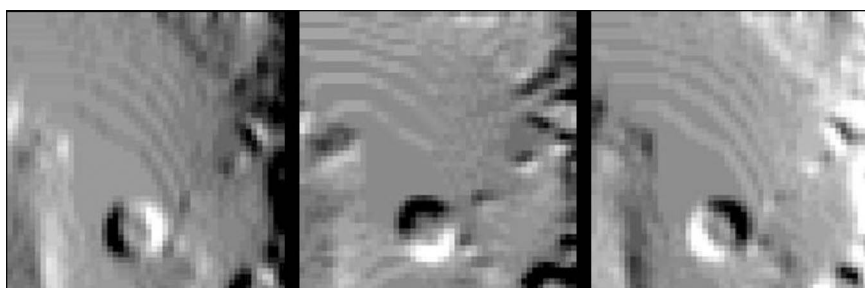


Figure 3. Level 1B VNIR radiance in RGB (red-green-blue) for the area of overlap between the daytime and nighttime TIR scenes from Fig. 2. R=band 3, G=band 2, and B=band 1. Yellow circles indicate fumaroles and yellow triangle shows a hot spring. Blue squares mark features of interest: 1- two fumaroles and an open pit mine in between; 2, 3, and 5 – rhyolite domes; 4 – dry lake.

at 11:52 a.m. daylight-saving time (i.e., 10:52 a.m. standard Pacific time). The nighttime scene was taken prior to the daytime scene, on 08/22/2001, at 11:06 p.m. daylight-saving time (i.e., 10:06 p.m. standard Pacific time and 6:06 a.m. on 08/23/2001 GMT time, hence the title of the nighttime scene in Figure 2). A subset of the VNIR scene covering the area of overlap between the daytime and the nighttime scenes in Figure 2 is shown in Figure 3.

The importance of taking into account the changing amount of heat through the course of a day is demonstrated in Figure 4. The scenes in Figure 4 zoom in on an area around a small topographic feature, a Quaternary rhyolite dome (diameter < 1 km), showing shaded relief at different times. It is evident that for any given pixel, depending on its location in respect to the local topography, the amount of solar heating



**Figure 4.** Example of changes in solar irradiation in the course of a day. Circular feature (rhyolite dome) is with a diameter  $\leq 1$  km. From left to right - shaded relief one hour after sunrise, 6 hours after sunrise/7 hours before sunset, and 4 hours before sunset.

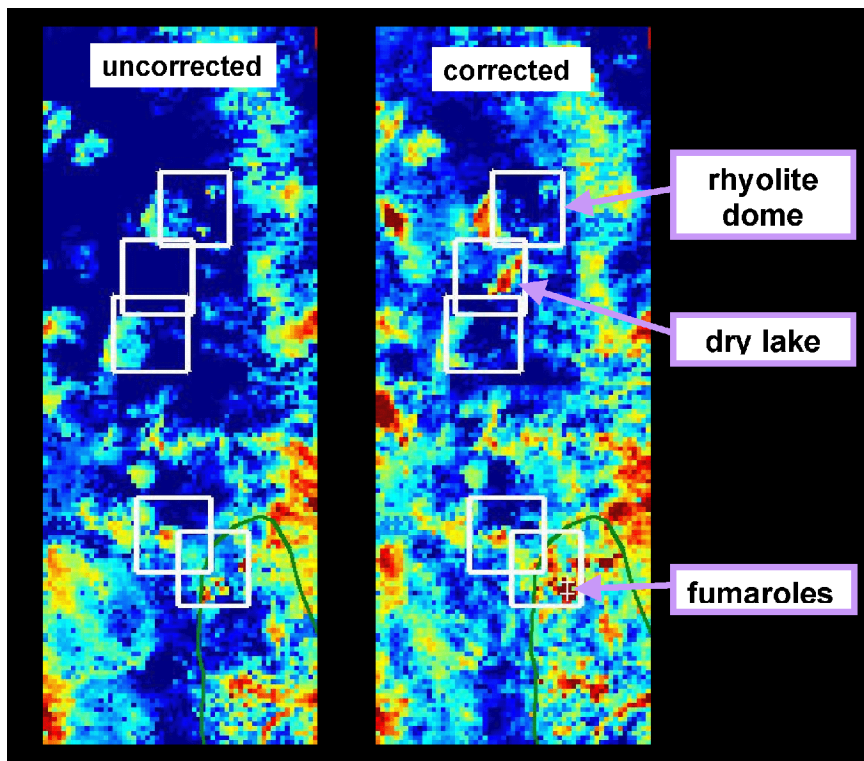


**Figure 5.** Comparison of the nighttime uncorrected and corrected AST\_08 images (surface temperature). White squares are the same as blue squares in Fig. 3. Note differences, especially around the two fumaroles and the dry lake, where elevated temperatures are only seen in the corrected image.

could be different from that received by adjacent pixels, and what is more, it changes during the day.

The simplified model described above approximately accounts for heat dissipation and was used to calculate pseudo-temperature images to be subtracted from the AST\_08 (surface temperature) images collected on 08/24/2001 (daytime) and 08/22/2001 (nighttime). The uncorrected and corrected nighttime AST\_08 (surface temperature) images are compared in Figure 5. The whole area is known to contain surface manifestations of geothermal energy, so it is not surprising that “red” (i.e., “hot”) areas are seen throughout the images. However, noise reduction is observed after correction and several features appear that are not seen in the uncorrected image (see caption to Figure 5). These results show that although simplified, the model applied here is potentially very effective in revealing and/or enhancing some thermal anomalies and suppressing false thermal anomalies.

One additional correction, for thermal inertia, was also performed (not shown). In this instance, the difference did not appear to be significant, but in principle, there may be cases when such corrections are very important.

## Future Work

Other than the issues of effects of topography, albedo, and thermal inertia, two other major effects need to be understood, those due to vegetation (e.g., Crippen and Blom, 2001) and atmospheric conditions (Finlayson-Pitts and Pitts, 1999; Tonooka, 2001). We are in the process of evaluating these effects and expect to develop a strategy to take them into account in the near future.

In addition to the limited data set of existing ASTER data, mostly collected in the daytime, we have made arrangements for future data collections over the next two years. These new data will emphasize nighttime TIR that are more suitable for the present type of studies. Several images will be collected per season, so that any spatially persistent thermal anomalies are reliably identified on the background of natural variability in the thermal data.

In the summer of 2006, we will carry out ground-based measurements, concurrently with the collection of a night/day pair of ASTER images over the Coso Geothermal Power Project. We intend to also collect measurements from a thermal infrared ground-based camera (FLIR), spectral measurements of albedo, and radiosonde measurements of atmospheric temperatures, water vapor and pressure, needed for atmospheric corrections. This field experiment is being organized with the participation of personnel from the Jet Propulsion Laboratory and the U. S. Navy Geothermal Program Office.

Furthermore, during the field experiment and using ASTER products in the optical range, we will attempt mineral mapping in order to provide independent or complementary markers for possible geothermal resources.

Finally, we will analyze the few existing airborne MASTER data collected over the region of interest in east central California and will endeavor to collect a more complete set of MASTER data in the future. The MASTER instrument was developed to simulate ASTER and another instrument on Terra, MODIS (Moderate Resolution Imaging Spectroradiometer). MASTER measures radiance in 50 channels between 0.4 and 13  $\mu\text{m}$ , 10 of which are TIR, with varying ground spatial resolution (5-20 meters) and swath (3.5-14 km), depending on flight altitude.

## Summary

- A rare day/night ASTER pair (1.5 day apart) covering partially the Coso KGRA was identified and analyzed for thermal anomalies associated with surface geothermal manifestations.
- Taking into account albedo, topographic and thermal inertia effects is very important in eliminating false thermal anomalies and revealing thermal signals not seen in the uncorrected imagery.
- Nighttime images and daytime pairs are currently being collected over the whole region of interest in east central California. This will make it possible to refine the heat model applied to the Coso images.
- Future analysis will be supported with field measurements of temperature and albedo at the Coso Geothermal Power Project.

## Acknowledgements

This project is funded by the California Energy Commission (CEC) and is partially matched by a NASA grant. Dr. William Glassely from CEC has provided continuous guidance and encouragement. A number of scientists at the Jet Propulsion Laboratory have been very helpful answering remote sensing questions (Dave Pieri, Mike Abrams, Greg Vaughan, Simon Hook, Frank Palluconi, Elsa Abbott) and making sure that future data are collected as intended (Leon Maldonado). LPDAAC staff has answered numerous questions related to the ASTER data.

## References

- Allis, R.G., G.D. Nash, and S.D. Johnson, 1999. "Conversion of Thermal Infrared Surveys to Heat Flow: Comparison from Dixie Valley, Nevada, and Wairakei, New Zealand." *Geothermal Resources Council Transactions*, v. 23, p. 499-504.
- Calvin, W., M. Coolbaugh, and R.G. Vaughan, 2002. "Geothermal Site Characterization Using Multi- and Hyperspectral Imagery." *Geothermal Resources Council Transactions*, v. 26, p. 483-484.
- Cochrane, G.R., M.A. Mongillo, P.R.L. Browne, and J.P. Derooin, 1994. "Satellite Studies of the Waimangu and Waiotapu Geothermal Areas, TVZ." In "Proceed. 16<sup>th</sup> NZ Geothermal Workshop," p. 181-198.
- Coolbaugh, M.F., 2003. "The Prediction and Detection of Geothermal Systems at Regional and Local Scales in Nevada using a Geographic Information System, Spatial Statistics, and Thermal Infrared Imagery." Ph.D. Thesis, University of Nevada Reno.
- Coolbaugh, M.F., J.V. Taranik, and F.A. Kruse, 2000. "Mapping of Surface Geothermal Anomalies at Steamboat Springs, NV using NASA Thermal Infrared Imaging Spectrometer (TIMS) and Advanced Visible and Infrared Imaging Spectrometer (AVIRIS) Data." In "Proceed. 14<sup>th</sup> Thematic Conf. Appl. Geologic Remote Sensing, Ann Arbor, MI," p. 623-630.
- Crippen, R., and R. Blom, 2001. "Unveiling the Lithology of Vegetated Terrains in Remotely Sensed Imagery." *Photogr. Eng. Rem. Sens.*, p. 935-944.
- Finlayson-Pitts, B.J., and J.N. Pitts, Jr., 1999. "Chemistry of the Upper and Lower Atmosphere: Theory, Experiments, and Applications." Academic Press, pp. 969.
- Martini, B.A., E.A. Silver, D.C. Potts, and W.L. Pickles, 2000. "Geological and Geobotanical Studies of Long Valley Caldera, CA, USA Utilizing New 5-m Hyperspectral Imagery." In "Proceed. IEEE Int. Geoscience Remote Sensing Symposium, July 2000."
- Monastero, F.C., 2002. "Model for Success: An Overview of Industry-Military Cooperation in the Development of Power Operations at the Coso Geothermal Field in Southern California." *Geothermal Resources Council Bulletin*, p. 188-194.
- Pickles, W.L., P.W. Kasameyer, B.A. Martini, D.C. Potts, and E.A. Silver, 2001. "Geobotanical Remote Sensing for Geothermal Exploration." *Geothermal Resources Council Transactions*, v. 25, p. 307-312.
- Sass, J., and S. Priest, 2002. "Geothermal California: California Claims the World's Highest Geothermal Power Output, with Potential for Even More Production with Advanced Techniques." *Geothermal Resources Council Bulletin*, p. 183-187.
- Tonoooka, H., 2001. "An Atmospheric Correction Algorithm for Thermal Infrared Multispectral Data Over Land—A Water-Vapor Scaling Method." *IEEE Transactions Geoscience Remote Sensing*, v. 39, p. 682-692.
- Williams, C.F., 2002. "Geothermal Systems of the Great Basin and U.S. Geological Survey Plans for a Regional Resource Assessment." *Geothermal Resources Council Transactions*, v. 26, p. 547-550.

